

Published in final edited form as:

Ann Thorac Surg. 2013 August ; 96(2): 586–595. doi:10.1016/j.athoracsur.2013.04.021.

Cardiac Surgical Delivery of the Sarcoplasmic Reticulum Calcium ATPase Rescues Myocytes in Ischemic Heart Failure

Anthony S. Fagnoli, MS, Michael G. Katz, MD, PhD, Charles Yarnall, CCP, Alice Isidro, PA-C, Michael Petrov, MD, Nury Steuerwald, PhD, Sriparna Ghosh, PhD, Kyle C. Richardville, BS, Richard Hillesheim, BS, Richard D. Williams, BS, Erik Kohlbrenner, BS, Hansell H. Stedman, MD, Roger J. Hajjar, MD, and Charles R. Bridges, MD, ScD

Sanger Heart & Vascular Institute, Carolinas Healthcare System, Charlotte, North Carolina; University of Pennsylvania School of Medicine, Philadelphia, Pennsylvania Cannon Research Center, Carolinas Healthcare System, Charlotte North Carolina Wiener Family Cardiovascular Research Laboratory, Mt. Sinai Medical Center, New York, New York

Abstract

Background—The sarcoplasmic reticulum calcium ATPase (SERCA2a) is an important molecular regulator of contractile dysfunction in heart failure. Gene transfer of SERCA2a mediated by molecular cardiac surgery with recirculating delivery (MCARD) is a novel and clinically translatable strategy.

Methods—Ischemic heart failure was induced by ligation of OM1 and OM2 in 14 sheep. Seven sheep underwent MCARD-mediated AAV1-SERCA2a delivery 4 weeks after myocardial infarction, and seven sheep served as untreated controls. Magnetic resonance imaging—based mechanoenergetic studies were performed at baseline, 3 weeks, and 12 weeks after infarction. Myocyte apoptosis was quantified by Tdt-mediated nick-end labeling assay. Myocyte cross-sectional area and caspase-8 and caspase-9 activity was measured with imaging software, specific fluorogenic peptides, and immunohistochemistry.

Results—MCARD-mediated AAV1-SERCA2a gene delivery resulted in robust cardiac-specific SERCA2a expression and stable improvements in global and regional contractility. There were significantly higher stroke volume index, left ventricular fractional thickening, and ejection fraction at 12 weeks in the MCARD group than in the control group (30 ± 3 vs 21 ± 2 mL/m²; $12\% \pm 5\%$ vs $3\% \pm 3\%$; and 43 ± 4 vs 32 ± 4 , respectively, all $p < 0.05$). Apoptotic myocytes were observed more frequently in the control group than in the MCARD-SERCA2a group ($0.57.2 \pm 0.16$ AU vs $0.32.4 \pm 0.08$ AU, $p < 0.05$). MCARD-SERCA2a also resulted in decreased caspase-8 and caspase-9 expression and decreased myocyte area in the border zone of transgenic sheep compared with control sheep ($14.6\% \pm 1.2\%$ vs $2.9\% \pm 0.7\%$; $18.2\% \pm 1.9\%$ vs $8.6\% \pm 1.4\%$; and 102.1 ± 3.8 μm^2 vs 88.1 ± 3.6 μm^2 , all $p < 0.05$).

Conclusions—MCARD-mediated SERCA2a delivery results in robust cardiac specific gene expression, improved contractility, and a decrease in both myocyte apoptosis and myocyte hypertrophy.

Recent advances in the understanding of the relevant molecular pathways, the evolution of gene transfer technology, and the development of recombinant viral vectors with significant

cardiac tropism facilitating long-term gene expression has made gene-based therapy an attractive approach for the treatment of ischemic heart failure (IHF).

One manifestation of failing myocytes is dysregulation of intracellular and extracellular calcium cycling and transport, which occurs by the sarcoplasmic reticulum (SR) calcium (Ca^{2+}) adenosine triphosphatase pump (SERCA2a) in both the systolic and diastolic phases. SERCA2a downregulation causes a prolongation of the Ca^{2+} transient, and it increases systolic and diastolic intracellular Ca^{2+} [1, 2]. Moreover, heart failure is consistently associated with a decreased expression level of SERCA2a and a reduction in activity [3–5].

Thus, the restoration of SERCA2a to normal levels in IHF is a rational treatment strategy. Currently, SERCA2a upregulation can best be achieved by use of vector-mediated gene delivery. Previous studies involving isolated failing myocytes and animal models of IHF have demonstrated that SERCA2a overexpression improves cardiac pump activity, normalizes calcium metabolism, and improves survival [6–8]. Yet, the relationship between apoptosis-induced myocyte loss, maladaptive remodeling in IHF, and SERCA mRNA expression after gene transfer has not been defined.

In this study we used molecular cardiac surgery with recirculating delivery (MCARD), a novel clinically translatable gene-delivery platform, to deliver adenoassociated virus (AAV1) encoding the SERCA2a transgene. We hypothesized that efficient MCARD-mediated delivery of SERCA2a in a large animal model of IHF would result in robust myocardial overexpression and have long-term beneficial effects on cardiac mechanoenergetics. We also endeavored to evaluate the effect of gene transfer on apoptosis, activation of different proteolytic caspases, and myocardial hypertrophy in the infarct border zone.

Material and Methods

All animals received humane care in compliance with guidelines established by the National Institutes of Health and by the Institutional Animal Care and Use Committee of the University of Pennsylvania. Concurrent with baseline magnetic resonance imaging (MRI), an ischemic infarction model was created in 14 sheep serving as time zero. The sheep were randomized into two groups: control (n = 7) and MCARD (n = 7), respectively. After infarction, sequential MRI studies were conducted 3 and 12 weeks after infarction. In contrast to the control group, which had no intervention, the MCARD group received 10^{13} GC of AAV1.CMV.SERCA2a 4 weeks after infarction. After sacrifice, molecular assays were conducted.

Surgical Procedures

INFARCT MODEL CREATION—One hour before infarct creation, a central venous amiodarone and lidocaine infusion was started. After thoracotomy, the proximal first and second branches of the circumflex artery were ligated. Electrocardiographic changes were noted, and the surrounding tissue discoloration confirmed infarct creation. The thoracotomy incision was closed.

MCARD—Surgical details of the MCARD procedure have been described previously [9, 10]. Briefly, after sternotomy, a transepical echocardiogram was performed. The right carotid artery was cannulated for systemic perfusion. The aortic root vent, superior vena cava (SVC) cannula, inferior vena cava (IVC) cannula, and retrograde cardioplegia catheter (coronary sinus) were placed, and cardiopulmonary bypass (CPB) was initiated. The right and left azygous (hemiazygous) veins were ligated. The left ventricular (LV), right ventricular (RV), and aortic root vents were connected to the cardiac venous return circuit.

The arterial limb of the cardiac circuit was connected to the coronary sinus catheter. The aorta was cross-clamped. Cold (4° C) crystalloid cardioplegia was delivered in an antegrade manner. The heart was isolated by tightening the SVC and IVC snares and cross-clamping the pulmonary artery. Retrograde cardiac circuit flow was initiated and maintained at 60 to 100 mL/min. The virus solution consisting of 10^{13} genome copies of AAV1.CMV.SERCA2a was infused into the retrograde coronary catheter and recirculated for 20 minutes. The circuit was then flushed to wash out residual vector. The aortic cross-clamp was removed, and rewarming was initiated. After the procedure, a transepical echocardiogram was performed.

Analysis of Cardiac Function and Hemodynamics

ELECTROCARDIOGRAPHY AND ECHOCARDIOGRAPHY—We performed electrocardiography in all animals before and after creation of myocardial infarction (MI) and analyzed the electrocardiogram to confirm segment elevation myocardial infarction. Transthoracic and transepical echocardiography was performed with a 7-MHz transducer (Acuson, Mountain View, CA) by using two-dimensional, spectral Doppler, and color flow Doppler modalities. A comprehensive assessment of cardiac structures and function was obtained.

MAGNETIC RESONANCE IMAGING ACQUISITION AND ANALYSIS—CINE cardiac series were generated for each animal at three time points (baseline, 3 weeks, and 12 weeks). LV pressure-gated images were recorded with a Millar catheter (Millar Instruments, Houston, TX). LV volumes over the cardiac cycle were obtained with the Segment Cardiac MRI software ([//segment.heiberg.se/](http://segment.heiberg.se/)). Pressure data from the Millar catheter were loaded into MATLAB 9.0 (Natick, MA), and built-in functions were used to calculate points for 15 to 30 consecutive pressure cycles.

Global and regional measures were obtained directly: stroke volume (SV), cardiac index (CI), end-diastolic volume index (EDVi), end-systolic volume index (ESVi), LV radial contraction velocity (RCV_{max}), LV fractional wall thickening (LV FWT), preload recruitable stroke work, and infarct size (%). Data points were indexed by body surface area, and analytic models were implemented to assess functional parameters [11].

AAV1/SERCA2a Production

A recombinant single stranded adenoassociated viral vector, serotype 1, encoding the human sarcoplasmic reticulum Ca^{2+} ATPase under the control of the human immediate early cytomegalovirus gene promoter with a splice donor/acceptor sequence and polyadenylation signal from the human-globin gene, was constructed in a validated preclinical grade system, resulting in high quality ssAAV1.CMV.SERCA2a titers [12].

Molecular Biology Assays for SERCA2a Expression

Quantitative polymerase chain reaction (QPCR) and reverse transcriptase polymerase chain reaction (RT-PCR) were performed. Briefly, high quality RNA and DNA were isolated from frozen specimens by use of the Chemagen MSM1 kits to set up separate RT-PCR and qPCR assays for SERCA2a mRNA and viral AAV1.CMV.SERCA2a DNA. To examine the expression of SERCA2a, customized kits designed by Abiomed Systems generated the following SERCA2a primers (forward 5' - tcaattacggggtcattagtc - 3' ; reverse 5' - ggagctacatctactagtagt - 3'). The level of ovine GAPDH RNA (forward: 5' - gcatcgtggagggactatga - 3' ; reverse: 5' - aagctgtggcgtgatggc - 3') was used to calculate normalized expression with the $\Delta\Delta Ct$ method for the RT-PCR values. Absolute genomic copies of SERCA2a DNA were quantified with the standard normal curve.

Definition of Infarct Border Zone

The border zone was defined by histology for tissue removal as follows: (1) The heart was removed and sectioned through the aorta, adjacent to the septum, to reveal the internal LV. (2) Scarred infarct zone was identified as discolored fibrous tissue. (3) Samples from a 1-cm zone extending from the outer discolored sections were taken as described previously [13]. For MRI analysis, gadolinium-delayed enhancement images were obtained, and the infarct zone was identified through pixel intensity algorithms [14]. Then, 20° to 30° sectors marked in the posterolateral wall anatomy zone were extended from the scar region to define the infarct border zone for regional LV analysis.

Myocardial Cell Apoptosis (TUNEL Assay)

Apoptosis detection in these sections was performed by the Tdt-mediated nick-end labeling (TUNEL) method with an apoptosis detection kit (Roche Diagnostics, Indianapolis, IN). Positive control was prepared with DNase. Negative control was obtained by omitting terminal transferase during the labeling procedure. Tissue specimens were evaluated by light microscopy and obtained from the infarct, border zone, and unaffected (remote) regions. The apoptotic rate was expressed as a ratio of the number of TUNEL-positive cardiomyocytes per nucleated cell per field.

Caspase Activity Assays

Tissue was fixed with 4% paraformaldehyde. Tissue sections were incubated with antirabbit primary antibodies for caspase 8 and 9 (1:1000). Goat antirabbit antibodies (1:1500) conjugated with Alexa 488 or 594 were used as secondary reagents. Nuclear DAPI staining was performed by premixed DAPI with proLong gold antifade mounting media. Fluorescence was visualized by a Zeiss LSM710 confocal microscope (Carl Zeiss GMBh, Jena, Germany) with ×63 objective. Image analysis was performed with the Zeiss ZEN 2010 image analysis software.

Cardiomyocyte Cross-Sectional Area

Paraffin-embedded LV sections were stained with hematoxylin and eosin. Microscopic fields were randomly selected from the LV. Each field was scanned together with a computer-generated microscale and analyzed with image-analyzing software by an observer who was blinded to the treatment group. No fewer than 50 cells per randomly chosen microscopic field were analyzed.

Remodeling Exclusion Criteria

The 3-week or pretreatment time point served as a benchmark to assess the degree of remodeling. We developed a normalized remodeling index score on the dimensions indexed by body surface area as follows: (1) pooled all 14 animals' variables, (2) applied statistical tests for normality in SPSS and Excel, and (3) fit each animal's ESV_i parameter at the 3-week time point to the normal curve (defined by all animals regardless of treatment group), obtaining a percentile score. We excluded outliers (percentile <5% or >95%) to remove animals with excessive or limited progression and to assure comparability of the groups.

Statistical Analysis

All data are presented as average \pm standard error of the mean. The Kolmogorov-Smirnov test for normality was applied to each data set. Single analysis of variance was performed across time (eg, baseline, 3 weeks, 12 weeks) for each parameter, then paired t tests ($p < 0.05$ significance) were used to assess any difference between any two time points or differences at the same time point between groups (eg, MCARD vs control).

Results

Survival and Inclusion Criteria

Three animals were excluded from the study. One animal (MCARD-SERCA2a group) died of refractory ventricular arrhythmias before the initiation of CPB, and two animals were excluded at the 3-week time point because one control animal presented with a very small infarct score (only one OM branch was present), and one animal was found to have rapid development of severe heart failure (EF less than 20%), requiring the daily use of diuretics and β -blockers in high doses. Both of these animals were excluded on the basis of the objective remodeling criteria described earlier (4th and 96th percentile, respectively). We analyzed the remaining six animals in the control group and five animals in the MCARD-SERCA2a group. LV infarct size measured by delayed enhancement MRI with gadolinium was similar between the control and MCARD-SERCA2a groups 3 weeks after MI ($16\% \pm 1\%$ vs $15\% \pm 2\%$, $p > 0.05$) and 12 weeks after MI ($17\% \pm 2\%$ vs $17\% \pm 2\%$, $p > 0.05$). In only two cases in the control group, we found mild (1+) MR. In all others there was no MR.

Biodistribution and Quantification of SERCA2a Gene Transfer and Expression

ABSOLUTE QUANTIFICATION OF SERCA2a GENOME COPIES WITH qPCR—MCARD-mediated SERCA2a gene delivery resulted in robust SERCA2a gene transfer, as indicated in the four LV regions. We found robust SERCA2a RNA expression levels in the LV lateral (border zone) and anterior walls: 4,300 and 4,200 GC per 100 ng DNA. These data are consistent with 0.24 and 0.23 SERCA2a GC/cell, whereas average collateral organ (liver) expression was 10.5-fold lower (0.025 GC/cell, $p < 0.05$). Moreover, in two cases liver expression was undetectable. These results clearly demonstrate MCARD's unique ability to achieve cardiac specificity with very high transfer levels in comparison with systemic tissues (Fig 1A).

RELATIVE QUANTIFICATION OF SERCA2a mRNA COPIES WITH RT-PCR—As found with the qPCR data, the RT-PCR values indicated a similar biodistribution in mRNA expression profile (Fig 1B).

MCARD-SERCA2a Gene Transfer and Cardiac Mechanics Assessment

GLOBAL LV FUNCTION—We assessed global cardiac function through CINE MRI images. The pretreatment data demonstrated no major differences between the control and MCARD-SERCA2a groups either at baseline or 3 weeks after MI. However, each group remodeled extensively, as evidenced by their significant loss of systolic and diastolic function from baseline to 3 weeks after MI (Table 1). Eight weeks after SERCA2a transfer (12 weeks after infarction), the hemodynamic data revealed significant amelioration of cardiac performance. The MCARD-SERCA2a group exhibited an increase in stroke volume index that was superior to the control group's 12-week results of 21 ± 2 mL/m² versus 30 ± 3 mL/m² ($p < 0.05$) and comparable with its own 3-week results ($p < 0.05$) (Fig 2A). Similarly, the MCARD-SERCA2a group had a higher ejection fraction at 12 weeks than did the control group ($43\% \pm 4\%$ vs $32\% \pm 4\%$, $p < 0.05$) (Fig 2B). Preload recruitable stroke work, a reliable load-independent index of intrinsic contractility, was preserved to a much greater extent from baseline in the MCARD-SERCA2a group (71 ± 9 erg/mL $\cdot 10^4$) than in the control group (51 ± 8 erg/mL $\cdot 10^4$). The control animals had a statistically significant increase in ESVi from 3 to 12 weeks (36 ± 2 mL/m²; 45 ± 3 mL/m², $p < 0.05$), whereas the MCARD-SERCA2a group did not (36 ± 5 mL/m²; 41 ± 6 mL/m², $p > 0.05$). Yet, EDVi increased to a similar degree in both groups. These data suggest that in the current dose range, SERCA2a gene transfer promotes a sustainable increase in systolic function without substantially improving diastolic remodeling.

REGIONAL LV FUNCTION—There were no significant differences between the control and MCARD groups at baseline in any parameter; however, key differences were noted at 12 weeks. The MCARD-SERCA2a group demonstrated superior fractional wall thickening in the posterolateral region ($12\% \pm 5\%$) compared with the control group ($3\% \pm 3\%$, $p < 0.05$) (Fig 3). Furthermore, the control group worsened from its baseline values ($19\% \pm 6\%$ vs $3\% \pm 3\%$, $p < 0.05$), whereas the MCARD-SERCA2a group ($24\% \pm 9\%$ vs $12\% \pm 5\%$) more stably retained function. In the ventricular infarct/border region, the MCARD-SERCA2a group presented with enhanced radial contraction velocity (13 ± 1 cm/s) in comparison with the control group (7 ± 3 cm/s) ($p < 0.05$), corroborating the positive changes found in global function.

MCARD-SERCA2a Gene Transfer, Myocardial Apoptosis, and Caspase Activity

TUNEL ASSAY—A TUNEL assay was performed to evaluate apoptosis in the infarcted area of the control group and the MCARD-SERCA2A group, as shown in Figure 4A. The frequency of TUNEL-positive cardiomyocytes was higher in the control group than in the MCARD-SERCA2A group (0.57 ± 0.16 AU vs 0.32 ± 0.08 AU, $p < 0.05$). No significant difference between the occurrences of TUNEL-positive cells was found in the remote zones in either group.

ACTIVATED CASPASE-8 AND CASPASE-9—Immunohistochemical detection of activated (cleaved) caspase-8 in cardiomyocytes confirmed the existence of apoptotic cells in the control group and the MCARD-SERCA2a group. SERCA2a treatment resulted in a significant decrease both in caspase-8 expression in the border zone of transgenic sheep ($14.6\% \pm 1.2\%$) compared with the control group ($18.2\% \pm 1.9\%$, $p < 0.05$) (Fig 4B) and in caspase-9 activity in transgenic sheep ($2.3\% \pm 1.0\%$) compared with the control group ($9.0\% \pm 3.0\%$, $p < 0.05$) (Fig 4C).

MCARD-SERCA2a gene transfer and myocardial hypertrophy

Myocyte cross-sectional area (an indication of cardiomyocyte hypertrophy) was significantly decreased in sheep treated with MCARD-SERCA2a compared with control sheep in the border zones of 12-week SERCA2a-treated sheep ($88.1 \pm 3.6 \mu\text{m}^2$) compared with $102.1 \pm 3.8 \mu\text{m}^2$ in control animals ($p < 0.05$) (Fig 4D).

Comment

Herein we have demonstrated detectable levels of human SERCA2a in all treated animals, with highest expression in the LV, including the border zone. Hence, improving border zone function may limit some of the negative effects of the infarct on myocardial function. Assessment of collateral organ gene expression indicates that there was relatively little transfer to the liver, assessed by qPCR, a biodistribution profile unique to MCARD. Separation of the cardiac circulation from the systemic circulation and the creation of a closed-loop recirculatory system increases gene transduction efficiency. To date, attempts to recapitulate a closed-loop configuration using catheter-based methods without CPB have failed [15, 16].

Furthermore, MCARD will potentially address the impact of preexisting neutralizing antibodies on AAV, eliminating up to 60% of patients from clinical gene therapy trials, including the Calcium Upregulation by Percutaneous Administration of Gene Therapy in Cardiac Disease (CUPID) trial [12, 17]. Unlike intracoronary delivery, MCARD effectively removes blood containing antibodies from the cardiac circulation. Moreover, by removing excess vector from the body, MCARD uniquely minimizes virus exposure to antigen-presenting cells, abrogating a T-cell-mediated immune response [9].

MCARD-SERCA2a overexpression and the associated preservation of calcium handling improved ventricular function in sheep with IHF represented by sustained LV contractility: significant improvements in SVi and CI; increased LV regional wall thickening; and maintenance of ejection fraction, radial contraction velocity, and PRSW. However EDV, and to a lesser extent ESV, continued to increase and were not substantially improved in comparison with the control group. In the current dose range, restoration of impaired calcium homeostasis and normalization of dysfunctional contractile responses after SERCA2a gene transfer does not completely reverse maladaptive remodeling. Nonetheless, our results support the hypothesis that SERCA2a gene transfer can restore impaired Ca^{2+} homeostasis and improve cardiac performance after myocardial infarction.

On the basis of experimental and clinical studies, CPB may induce apoptosis with generation of oxygen free radicals and cytokine release. According to most authors, the number of apoptotic cells is increased after CPB [18]. Thus, the absence of CPB in the control group would not account for the observed increase in apoptosis.

Heart failure is characterized by adverse structural changes with cardiac remodeling. This process is associated with myocardial hypertrophy followed by an absolute reduction in the number of cardiomyocytes. During ischemia and the subsequent transition to heart failure in animal models and humans, as many as 30% to 50% of cardiac myocytes in the area at risk undergo dedifferentiation and eventually apoptosis. In this study we analyzed both apoptotic pathways in our model of IHF and how each is modified after gene delivery. The results suggest that (1) activation of both caspases takes place with decompensated heart failure and (2) SERCA2a overexpression ameliorates both the mitochondrial pathway (caspase 9) and the extrinsic pathway (caspase 8).

Hypertrophy of the LV is considered to be a compensatory phenomenon of cardiac remodeling. The transition from compensated concentric hypertrophy to decompensated eccentric hypertrophy is associated with an increased number of apoptotic myocytes. Our data demonstrate that SERCA2a may be an important regulator of cardiac hypertrophy. SERCA2a-induced regression of myocyte hypertrophy may be mediated through regulation of the Ca^{2+} -regulating serine/threonine phosphatase, calcineurin, which plays a central role in hypertrophic growth in cardiac muscle. We hypothesize that increased SERCA2a activity stimulates SR Ca^{2+} uptake, thereby diminishing intracellular Ca^{2+} , which leads to downregulation of the calcineurin/nuclear factor of activated T cells signaling pathway [19].

Clinically, MCARD-mediated gene delivery would be applicable to (1) patients with moderate to severe LV dysfunction who would undergo cardiac operations for other reasons; (2) 35% of patients in whom intracoronary delivery would be contraindicated because of chronic total coronary occlusion; (3) patients with genetic factors responsible for up to 50% of dilated cardiomyopathy, particularly those with an X-linked or autosomal recessive inheritance pattern; and (4) patients with neutralizing antibodies to AAV. MCARD may also be an ideal method for cardiac stem cell delivery, particularly in patients with coronary occlusive disease who are currently excluded from clinical trials [20]. The MCARD procedure can readily be adapted for minimally invasive or robotic operations.

There are several limitations to this study. We used the same dose of vector as in the high-dose cohort in the CUPID trial [12] without a dose response. We did not incorporate a true control group with MCARD-null vector because of the high time and material cost of this group. This limitation notwithstanding, we thought it unlikely that CPB or null vector alone (MCARD-null) would result in the benefits observed, although we cannot explicitly exclude this possibility.

In conclusion, we believe that the most significant need in preclinical trials is to establish what level of transfer is required with a consistent delivery method to achieve clinical benefit. Closed-loop recirculating methods like MCARD would offer a unique solution for the clinic and would usher in the concept of targeted transvascular delivery. We found that the use of a SERCA2a gene therapy strategy inhibits apoptotic pathways, decreases myocardial hypertrophy, and is associated with improvement of systolic myocardial function.

Acknowledgments

This study was supported by National Institutes of Health grant 1-R01 HL083078-01A2 (C.R.B.). We acknowledge the NHLBI Gene Therapy Resource Program. The authors thank Catherine Tomasulo, Louella Pritchette, and Marina Sumaroka for technical assistance; James J. Pilla and Ted Plappert for MRI and echocardiography; Jane Ingram, Natalia Zinchenko, and Amber Smith for histology; Einar Heiberg for MRI software; and the veterinarians and veterinary technicians of the University of Pennsylvania.

References

1. Gwathmey JK, Copelas L, MacKinnon R, et al. Abnormal intracellular calcium handling in myocardium from patients with end-stage heart failure. *Circ Res.* 1987; 61:70–6. [PubMed: 3608112]
2. Hasenfuss G, Pieske B. Calcium cycling in congestive heart failure. *J Mol Cell Cardiol.* 2002; 34:951–69. [PubMed: 12234765]
3. Piacentino V III, Weber CR, Chen X, et al. Cellular basis of abnormal calcium transients of failing human ventricular myocytes. *Circ Res.* 2003; 92:651–8. [PubMed: 12600875]
4. del Monte, Hajjar RJ. Intracellular devastation in heart failure. *Heart Fail Rev.* 2008; 13:151–62. [PubMed: 18347978]
5. Tilemann L, Ishikawa K, Weber T, Hajjar RJ. Gene therapy for heart failure. *Circ Res.* 2012; 110:770–93.
6. Muller OJ, Lange M, Rattunde H, et al. Transgenic rat hearts overexpressing SERCA2a show improved contractility under baseline conditions and pressure overload. *Cardiovasc Res.* 2003; 59:380–9. [PubMed: 12909321]
7. Rapti, K.; Hajjar, RJ.; Weber, T. Novel approaches to deliver molecular therapeutics in cardiac disease using adeno-associated virus vectors. In: Coleman, WB.; Tsongalis, GJ., editors. *Translational cardiology.* Springer; New York: 2012. p. 391-458.
8. del Monte F, Williams E, Lebeche D, et al. Improvement in survival and cardiac metabolism after gene transfer of sarcoplasmic reticulum Ca (2+)-ATPase in a rat model of heart failure. *Circulation.* 2001; 104:1424–9. [PubMed: 11560860]
9. White JD, Thesier DM, Swain JB, et al. Myocardial gene delivery using molecular cardiac surgery with recombinant adeno-associated virus vectors in vivo. *Gene Ther.* 2011; 18:546–52. [PubMed: 21228882]
10. Katz MG, Fargnoli AS, Swain JD, et al. AAV6-BARKct gene delivery mediated by molecular cardiac surgery with recirculating delivery in sheep results in robust gene expression and increased adrenergic reserve. *J Thorac Cardiovasc Surg.* 2012; 143:720–6. [PubMed: 22143102]
11. Feneley MP, Skelton TN, Kisslo KB, Davis JW, Bashore TM, Rankin JS. Comparison of preload recruitable stroke work, end-systolic pressure-volume and dP/dtmax-end-diastolic volume relations as indexes of left ventricular contractile performance in patients undergoing routine cardiac catheterization. *J Am Coll Cardiol.* 1992; 19:1522–30. [PubMed: 1593048]
12. Jessup M, Greenberg B, Mancini D, et al. Calcium Upregulation by Percutaneous Administration of Gene Therapy in Cardiac Disease (CUPID): a phase 2 trial of intracoronary gene therapy of sarcoplasmic reticulum Ca²⁺-ATPase in patients with advanced heart failure. *Circulation.* 2011; 124:304–13. [PubMed: 21709064]
13. Driesen RB, Verheyen FK, Dijkstra P, et al. Structural remodeling of cardiomyocytes in the border zone of infarcted rabbit heart. *Mol Cell Biochem.* 2007; 302:225–32. [PubMed: 17387581]

14. O'Regan DP, Ahmed R, Neuwirth C, et al. Cardiac MRI of myocardial salvage at the peri-infarct border zones after primary coronary intervention. *Am J Physiol Heart Circ Physiol*. 2009; 297:H340–6. [PubMed: 19429834]
15. Byrne MJ, Power JM, Prevolos A, et al. Recirculating cardiac delivery of AAV2/1SERCA2a improves myocardial function in an experimental model of heart failure on large animals. *Gene Ther*. 2008; 15:1550–7. [PubMed: 18650850]
16. Bridges CR. Recirculating cardiac delivery method of gene delivery should be called non-recirculating method. *Gene Ther*. 2009; 16:939–40. [PubMed: 19340020]
17. Rapti K, Louis-Jeune V, Kohlbrenner E, et al. Neutralizing antibodies against AAV serotypes 1,2,6 and 9 in sera of commonly used animal models. *Mol Ther*. 2012; 20:73–83. [PubMed: 21915102]
18. Valen G. The basic biology of apoptosis and its implications for cardiac function and viability. *Ann Thorac Surg*. 2003; 75:S656–60. [PubMed: 12607708]
19. Lipskaia L, Chemaly ER, Hadri L, et al. Sarcoplasmic reticulum Ca²⁺ ATPase as a therapeutic target for heart failure. *Expert Opin Biol Ther*. 2010; 10:29–41. [PubMed: 20078230]
20. Makkar RJ, Smith RR, Cheng Ke, et al. Intracoronary cardiosphere-derived cells for heart regeneration after myocardial infarction (CADUCEUS): a prospective, randomized phase 1 trial. *Lancet*. 2012; 379:895–904. [PubMed: 22336189]

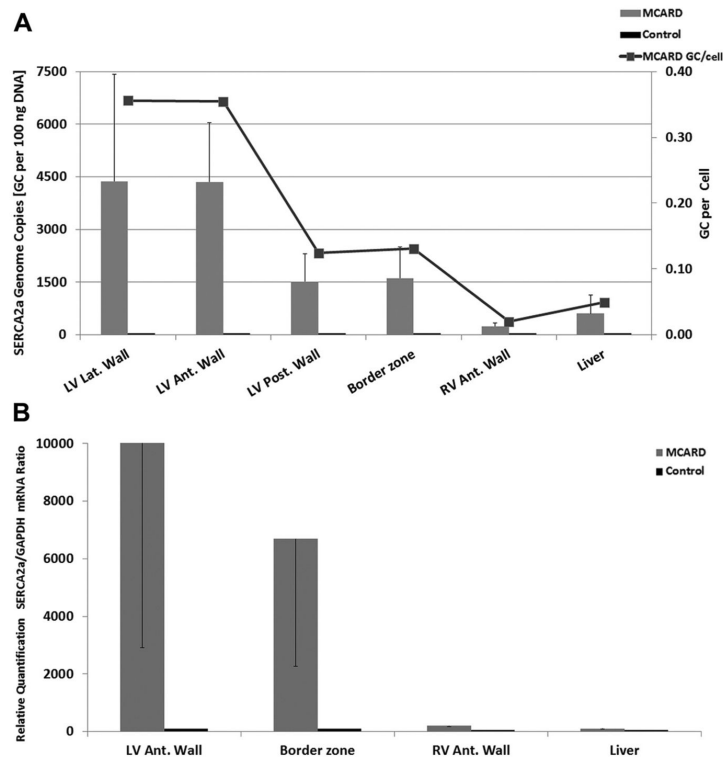


Fig. 1. (A) Molecular cardiac surgery with recirculating delivery (MCARD)-mediated sarcoplasmic reticulum Ca^{2+} adenosine triphosphatase (SERCA2a) DNA expression at 12 weeks: quantitative polymerase chain reaction (PCR) results of adeno-associated virus sarcoplasmic reticulum calcium adenosine triphosphatase pump (AAV1.-SERCA2a) gene transfer. (B) MCARD-mediated SERCA2a mRNA expression at 12 weeks: reverse transcription (PCR) results of AAV1.SERCA2a gene transfer.

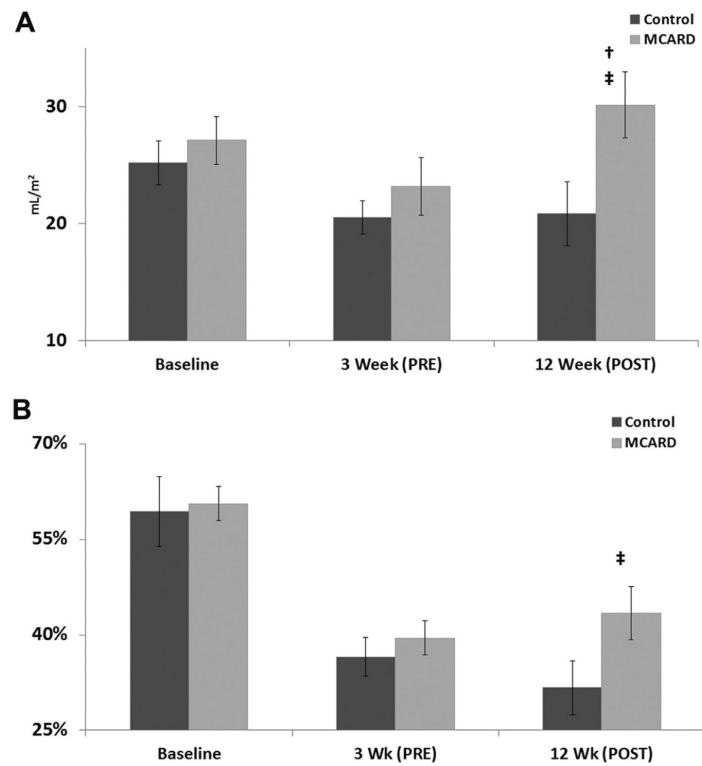


Fig. 2. (A) Changes in stroke volume index (mL/m²) over time. †p<0.05 for difference from 3-week to 12-week time points in either the control group or the molecular cardiac surgery with recirculating delivery (MCARD) group. ‡p<0.05 for difference between MCARD and control groups at 12 weeks. (B) Changes in ejection fraction (%) over time. †p<0.05 for difference from 3-week to 12-week time points in either the control group or the MCARD group. ‡p<0.05 for difference between MCARD and control groups at 12 weeks.

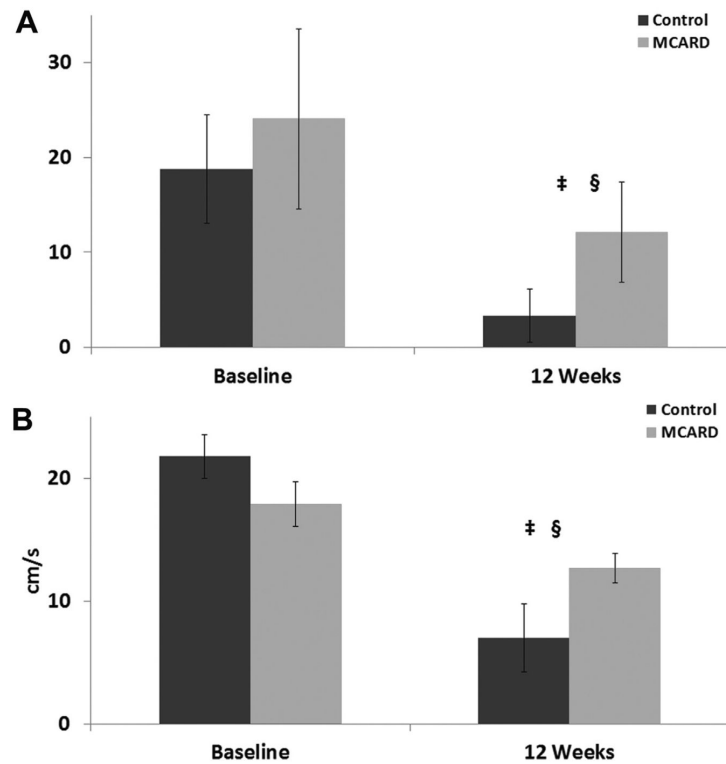


Fig. 3. (A) Changes in basal region left ventricular fractional thickening (%) over time. $§p < 0.05$ for difference from baseline to 12-week time points in either the control group or the molecular cardiac surgery with recirculating delivery (MCARD) group. $‡p < 0.05$ for difference between MCARD and control groups at 12 weeks. (B) Changes in middle region left ventricular radial contraction velocity (cm/s) over time. $§p < 0.05$ for difference from baseline to 12-week time points in either the control group or the MCARD group. $‡p < 0.05$ for difference between MCARD and control groups at 12 weeks.

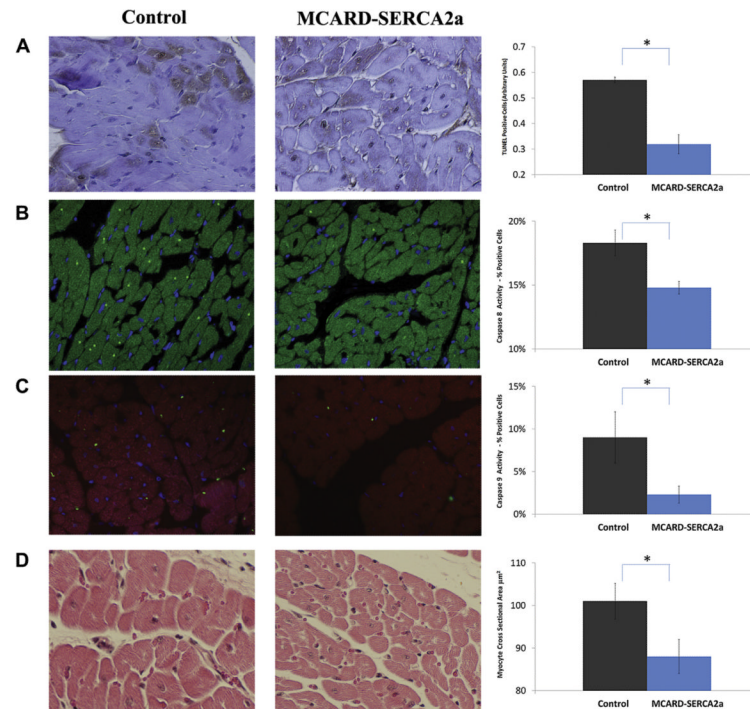


Fig. 4. (A) Quantitative immunohistochemistry-apoptosis staining of control group vs molecular cardiac surgery with recirculating delivery (MCARD) group (brown area indicates apoptosis). Magnification: $\times 400$. (B) Quantitative confocal microscopy of caspase 8 biomarker of control vs MCARD (bright green dot indicates positive nuclei). Magnification: $\times 400$. (C) Quantitative confocal microscopy of caspase 9 biomarker of control vs MCARD (bright green dot indicates positive nuclei). Magnification: $\times 400$. (D) Quantitative left ventricular myocyte cross-sectional area of control vs MCARD. Magnification: $\times 400$. *Indicates $p < 0.05$ between control and MCARD groups. All samples were obtained from the infarct border zone 12 weeks after myocardial infarction. TUNEL = Tdt-mediated nick-end labeling.

Table 1

Summary of Hemodynamic and Energetics Data

Global LV Mechanics	Baseline			3 Weeks After MI			12 Weeks After MI		
	Control	MCARD	<i>p</i> Value	Control	MCARD	<i>p</i> Value	Control	MCARD	<i>p</i> Value
Weight (kg)	42 ± 2	42 ± 1	0.49	43 ± 2	41 ± 1	0.25	49 ± 2	45 ± 1	0.06
Heart rate (beats/min)	101 ± 3	100 ± 4	0.42	96 ± 5	84 ± 5	0.08	91 ± 6	79 ± 5	0.07
Mean systolic pressure (mm Hg)	86 ± 5	90 ± 5	0.29	83 ± 5	79 ± 4	0.31	87 ± 9	81 ± 7	0.30
LV infarct size (%)	N/A	N/A	N/A	16 ± 1	15 ± 2	0.34	17 ± 2	17 ± 2	0.45
EDVi (mL/m ²)	45 ± 2	45 ± 2	0.49	58 ± 3	59 ± 7	0.42	66 ± 2	71 ± 7	0.21
ESVi (mL/m ²)	19 ± 3	18 ± 1	0.36	36 ± 2	36 ± 5	0.49	45 ± 3	41 ± 6	0.29
SVi (mL/m ²)	26 ± 2	27 ± 2	0.35	22 ± 2	23 ± 2	0.29	21 ± 2	30 ± 3	0.02
EF (%)	59 ± 5	61 ± 2	0.38	38 ± 3	40 ± 3	0.26	32 ± 4	43 ± 4	0.03
CI (mL/min · m ²)	2,596 ± 137	2,676 ± 113	0.35	2,070 ± 96	1,976 ± 283	0.37	1,862 ± 93	2,352 ± 187	0.02
dP/dt _{MAX} (mm Hg/s)	1,128 ± 126	1,151 ± 92	0.43	986 ± 114	1,121 ± 184	0.29	1,073 ± 147	854 ± 152	0.30
dP/dt _{MIN} (mm Hg/s)	-1,362 ± 84	-1,769 ± 217	0.07	-1,300 ± 143	-1,544 ± 297	0.26	-1,355 ± 112	-1,776 ± 509	0.33
PRSW (erg · mL ⁻¹ · 10 ⁴)	89 ± 7	94 ± 10	0.35	69 ± 9	67 ± 10	0.42	51 ± 8	71 ± 9	0.07
Regional LV mechanics: posterolateral wall region^a									
	Control	MCARD	<i>p</i> Value	Control	MCARD	<i>p</i> Value	Control	MCARD	<i>p</i> Value
Frac. wall thickening (%)	19 ± 6	24 ± 9	0.34	5 ± 6	6 ± 5	0.44	3 ± 3	12 ± 5	0.04
ES wall thickness (mm)	11 ± 1	13 ± 1	0.07	8 ± 1	9 ± 1	0.46	7 ± 1	8 ± 1	0.20
Radial velocity _{MAX} (cm/s)	22 ± 2	18 ± 2	0.09	15 ± 3	13 ± 3	0.38	7 ± 3	13 ± 1	0.04

CI = cardiac index; dP/dt = first derivative of the left ventricular intracavitary pressure; EDVi = end diastolic volume index; EF = ejection fraction; ES = end systolic; ESVi = end systolic volume index; Frac. = fractional; LV = left ventricle; MCARD = molecular cardiac surgery with recirculating delivery; MI = myocardial infarction; PRSW = preload recruitable stroke work; SVi = stroke volume index.

Shaded values indicate significance at $p < 0.05$ level.

^aPosterolateral wall region includes infarct and border zone within or remote zone.